Practical Approach to the Prediction of Rutting in Asphalt Pavements: The Shell Method

P. J. van de Loo, Koninklijke/Shell-Laboratorium, Amsterdam

This paper describes a true engineering method for predicting rut depth. It demonstrates how a mix design procedure based on creep testing can be used as a subsystem in an overall pavement management system. The proposed system makes it possible to calculate the decline in riding quality of a pavement as a function of time caused by permanent deformation. It is shown that (a) the service life of a pavement can be related to the bitumen properties, (b) the mix properties can be given as a function of the bitumen properties, (c) the total number of wheel loads of a given wheel-load spectrum can be expressed as an equivalent number of standard wheel loads, depending on the mix characteristics, (d) the influence of a varying contact area between the tire and the pavement is negligible in the case of a proper choice of the standard wheel, (e) the lateral distribution of wheel loads over the traffic lane and the occurrence of lateral swellings result in rut depth values (top to bottom) that are approximately equal to the reduction in layer thickness caused by the equivalent number of standard wheels in a single wheel path, and (f) the temperature variations must be corrected for by a proper calculation of average viscosities.

In the continuous struggle against the deterioration of asphalt pavements the emphasis is sometimes on cracking and sometimes on permanent deformation. In areas in which permanent deformation or rutting is regarded as the more serious problem, the mix design has often been based on Marshall stability criteria. Although this frequently leads to improvements because extremely unstable mixes are rejected, the results are not satisfactory in all respects. In the first place, too many pavements still show rutting, even after the use of a Marshall test procedure. In the second place, as has been confirmed recently in Germany (1) and Holland (2), the reproducibility of the test itself is relatively poor. Moreover, the test procedure was originally developed for asphaltic concrete mixes and is not necessarily applicable to other types of mixes. Furthermore, the quantities measured cannot easily be interpreted directly in engineering terms, but derive their significance mainly from experience with such test results. This can be an important disadvantage, in particular when unconventional materials or mix compositions or both require evaluation and there is little or no experience in their use. The main problem, however, is the fact that the measured quantities cannot be incorporated into a calculation procedure for the overall design of a pavement structure. Therefore, a new method for mix evaluation has been developed (3, 4, 5, 6).

In a pavement management system it is necessary to predict how the riding quality of the pavement will deteriorate as a function of time. One of the factors that influences the riding quality, and therefore the service life of a pavement, is permanent deformation. In several countries an overlay is applied when the rut depth is of the order of 20 to 30 mm. For this reason a complete pavement management system must contain a subsystem with which to calculate or predict rut depth.

In this paper a pavement management subsystem for calculating the rut depth at a given service life is presented. It is restricted to rutting caused by deformation in the asphalt layer, assuming that deformations in the unbound layers underneath can be avoided by a proper thickness design. In the absence of such a thickness design, the deformations in the unbound layers must be added to that in the asphalt. The paper describes the basic principles of the system, defines the problem areas, and discusses possible solutions (these depend mainly on the accuracy required). However, since many of the other factors that influence the riding quality of a pavement cannot be predicted with a high degree of accuracy, the individual investigator must set his own standards of accuracy for predicting rut depth.

BASIC SYSTEM FOR PREDICTING PERMANENT DEFORMATION

For ease of expression, the basic system will be explained here by referring to a single wheel load that moves in a single wheel path without lateral movements (i.e., a laboratory test track study). More practical conditions, such as wheel-load spectra, varying contact areas between tires and pavements, lateral distributions of wheels over the traffic lane, and large temperature gradients in the asphalt layer, will be considered in the next section.

Publication of this paper sponsored by Committee on Strength and Deformation Characteristics of Pavement Sections.

The design system will be outlined with the flow diagram shown in Figure 1; successive steps in the simplified procedure are numbered according to this figure.

In the design of a pavement or an overlay, the factors to be considered are the conditions at the site, the traffic to be expected, weighted by its intensity and the wheel-load distribution, and the climatic conditions (step 1). The asphalt layer thickness H_0 can then be calculated on the basis of these quantities. The criteria for this include a maximum permissible compressive strain at the top of the subgrade and a maximum permissible horizontal strain at the bottom of the asphalt layer. The dynamic modulus of the asphalt, which is needed for the calculations, can be measured directly or estimated from existing data (step 2).

The rutting that will occur in a pavement depends on the average stress in the asphalt mix under the moving wheel, which may be calculated with the elastic-layer computer program BISAR, an extension of the BISTRO program (7, 8). Figure 2 shows Z, the proportionality factor between the average stress and the contact stress (between the tire and pavement), calculated for the simplest case of a full-depth asphalt construction (4) (step 3). From a given wheel load and a given contact area, and the known quantities (H_0, E, E_∞, μ, μ_∞), the applicable Z-value can be determined from this figure (step 4).

In order to calculate the rut depth in the design life of a pavement, the parameters listed in step 1 must relate to the material properties. The viscosity nomograph [Figure 3 (4)] shows the bitumen viscosity as a function of $T - T_{800\ pen}$, the difference between the bitumen temperature and the temperature at which the penetration value is equal to 800 (9), with the penetration index (PI) as a parameter. It covers the range of temperatures that may be present in a pavement. The viscosity as a function of the pavement temperature can be derived from this nomograph, if the bitumen properties are known (step 5).

Since it is assumed that permanent deformation or rutting is a function of only the viscous or nonelastic component of the bitumen stiffness ($S_{bit,\,visc}$), the service life of a pavement may be expressed as (step 6)

$$S_{bit,\,visc} = 3 \Big/ \sum_{T,t_0} (N\, t_0/\eta) \qquad (1)$$

where

N = total number of wheel passes,
t_0 = loading time of one wheel pass, and
η = bitumen viscosity.

The bitumen viscosity is defined as

Figure 1. Pavement management subsystem for calculation of reduction in layer thickness at a given service life.

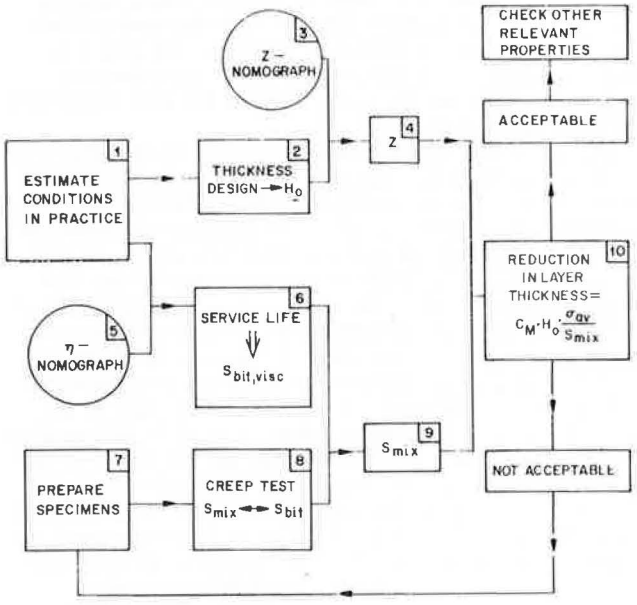

Figure 2. Relation between Z and R/H_0 derived from BISAR analysis of the elastic layer model ($\mu = \mu_\infty = 0.35$).

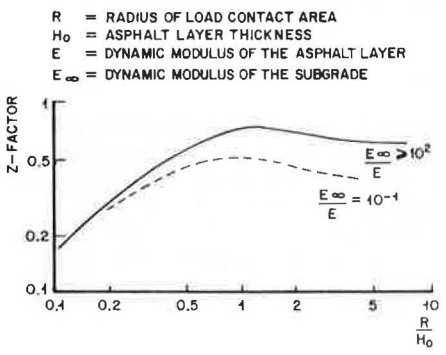

Figure 3. Viscosity of bitumen as a function of $(T - T_{800\ pen})$ and PI.

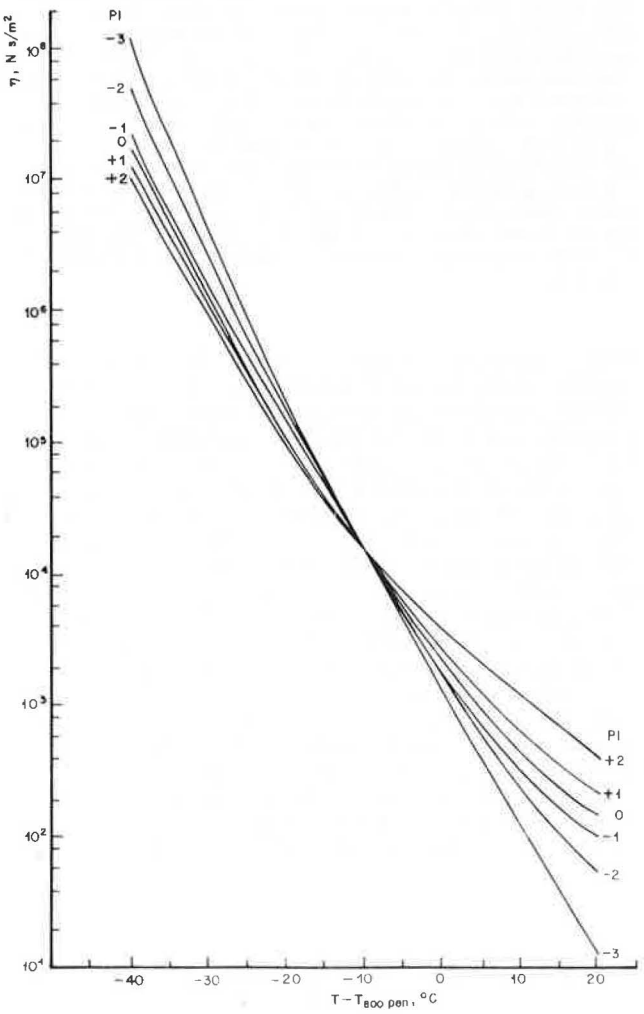

$$\eta = \tfrac{1}{3} \lim_{t \to \infty} S_{bit}\, t \qquad (2)$$

The experimental part of the procedure requires that the laboratory method of mixing and compaction of the specimens should be as close to the field method as possible: There must be at least a correlation between the mechanical properties obtained in the laboratory and those obtained in the field. In general, this problem is common to all test methods and is not unique to creep testing. The laboratory specimens are then studied by the unconfined constant-load creep compression test (step 8) (3, 4, 5), which measures a mix characteristic, in which the stiffness modulus of the mix (S_{mix}) is derived as a function of the stiffness modulus of the bitumen (S_{bit}). From the mix characteristic, S_{mix} is derived at the value of S_{bit} equal to $S_{bit,\,visc}$, which has been calculated from the design life of the pavement (step 9).

Finally, the reduction in layer thickness can be calculated (step 10):

$$\text{reduction in layer thickness} = C_M H_0 \sigma_{av}/S_{mix} \qquad (3)$$

where

- C_M = correction factor for the so-called dynamic effect, which takes account of differences between static (creep) and dynamic (rutting) behavior [this factor depends on the type of mix and must be determined empirically (5)],
- H_0 = design thickness of the asphalt layer,
- σ_{av} = average stress in the pavement under the moving wheel, and
- S_{mix} = value of the stiffness of the mix at $S_{bit} = S_{bit,\,visc}$, which was derived in step 9.

$$\sigma_{av} = Z\sigma_0 \qquad (4)$$

where Z has been derived from Figure 4, and σ_0 is the contact stress between tire and pavement.

However, it is not the reduction in layer thickness, but the total rut depth that is relevant for the riding quality of a pavement. The rut depth is defined as the difference in height between the top of a lateral swelling and the lowest point inside a rut; if no aftercompaction occurs, the material that is pushed away in the rut will appear as a lateral swelling. From observations on many test tracks, the rut depth is about 1.5 times the reduction in layer thickness.

This calculation procedure will give a value for the reduction in layer thickness that may be acceptable or unacceptable. If the value is too high, the mix composition should be changed and the procedure repeated. If the calculated reduction is acceptable, then the other relevant properties, such as resistance to fatigue, breaking strength, and durability, should be investigated. The above-described procedure has been applied to a number of different mixes tested on various test tracks. Agreement was within a factor of 2 (4, 5) without the empirical correction factor C_M and better with the application of proper C_M values.

EXTENSION TO PRACTICAL CONDITIONS

The problems related to the application of the principles discussed above to the practical cases of varying wheel loads and contact areas, lateral distribution over the traffic lane, and varying temperatures will be discussed below.

Wheel-Load Spectrum

Experiments on laboratory test tracks are generally carried out with a single, constant wheel load. In practice, traffic is composed of light and heavy vehicles, and the influence of the total wheel-load spectrum must be taken into account. In rutting studies the load spectrum is expressed as the contact stress between the tire and the pavement. This section introduces some simplifications that do not influence the principles of the theory.

The wheel-load spectrum (Figure 4) is replaced by the simplified wheel-load spectrum (Figure 5), which consists of N_1 wheel passes with contact stress σ_1 and N_2 wheel passes with stress σ_2. The sequence of loading is random (Figure 6). The load spectrum may then be divided into a number of repeated block loadings, in which σ_1 and σ_2 are represented in the ratio n_1/n_2 (= N_1/N_2). Within such a block, loadings with equal σ are taken together (Figure 7). The sequence of the applications of σ_1 and σ_2 may influence the deformation level, but at an increasing number of repeated block loadings this influence diminishes.

Next, the influence of the simplified wheel-load spectrum on the permanent deformation or rut depth is studied. The rutting characteristic, in which the rut depth ϵ_p is given as a function of the number of wheel passes N, depends on the contact stress between the tire and the asphalt surface. A wheel load with a constant σ follows a single curve. However, a sequence of different loadings cannot be represented by a single curve. During the course of a deformation process the material continuously changes its properties: The resistance to permanent deformation increases, i.e., $d\epsilon/dN$ decreases. The magnitude of this decrease depends on σ. In view of this continuous change, it is not correct to simply add up the deformations caused by N_1 loads of σ_1 and N_2 loads of σ_2. Therefore, the following assumption is made: The material can be characterized by its state of deformation or deformation level, regardless of the way in which this state has been obtained.

The required compound block loading procedure is described as follows: When n_i loads of σ_i are applied, and a preceding arbitrary load pattern has caused a rut depth ϵ_p, then the rutting curve from σ_i must be followed by n_i load applications of σ_i, beginning at level ϵ_p. In Figure 8 this procedure is illustrated for n_1, σ_1 and n_2, σ_2. To fix the final deformation level the procedure must be repeated almost infinitely. Only if the ϵ-N relationship is known in analytical form, is it possible to calculate the final deformation level.

For many of the asphalt mixes tested, the strain in the mix is proportional to the applied stress (linearity).

$$\epsilon = f_1(\sigma, N) = \sigma\, f(N) \qquad (5)$$

In most cases, the functional relationship between ϵ and N can be described with sufficient accuracy by a linear log-log relationship (Figure 9):

$$\epsilon = c\sigma N^a \qquad (6)$$

Now, if n_1 loads σ_1 and n_2 loads σ_2 are applied alternately, the simplest procedure for the study of the influence on rut depth will be to determine the equivalent number of standard loads that would cause the same rut depth as the compound loading, i.e., to determine n_{st} that causes the same increase in rut depth $d\epsilon_{st}$ as is caused by n_i loads of σ_i.

Assume that, after an arbitrary load history, the permanent deformation is ϵ_p. From the standard curve, this level would be obtained after N_{st} wheel loads or from the σ_i curve, after N_i wheel loads. From equation 6 it follows that

$$N_{st} = (\epsilon_p/c\sigma_{st})^{1/a} \qquad (7)$$

$$N_i = (\epsilon_p/c\sigma_i)^{1/a} \qquad (8)$$

or

$$N_{st} = (\sigma_i/\sigma_{st})^{1/a} N_i \quad (9)$$

This equation gives the equivalent number of standard loads causing the same deformation ϵ_p as N_i loads σ_i. However, at equal ϵ_p, $d\epsilon/dN$ differs for the different σ curves and is a function of N, i.e.,

$$d\epsilon/dN = c\sigma a N^{a-1} \quad (10)$$

or

$$d\epsilon/dN = \epsilon_p\, a/N \quad (11)$$

for the standard curve:

$$d\epsilon_{st} = \epsilon_p\, (a/N_{st})\, dN_{st} \quad (12)$$

for the σ_i curve:

$$d\epsilon_i = \epsilon_p\, (a/N_i) dN_i \quad (13)$$

Put $dN_i = n_i$ and calculate $dN_{st} = n_{st}$ for the case in which the increases in deformation along both curves are equal.

$$d\epsilon_{st} = d\epsilon_i \quad (14)$$

$$\epsilon_p\, (a/N_{st})\, n_{st} = \epsilon_p\, (a/N_i)\, n_i \quad (15)$$

$$n_{st} = (N_{st}/N_i)\, n_i \quad (16)$$

Substitute equation 7 and 8 into equation 16.

$$n_{st} = (\sigma_i/\sigma_{st})^{1/a}\, n_i \quad (17)$$

Equation 17 is similar to equation 9. This means that, for any load pattern, the equivalent number of standard loads can be determined, not only in the case of a certain deformation level obtained, but also for the incremental deformations, regardless of the fact that $d\epsilon/dN$, or the measure of increasing resistance to permanent deformation, differs for the various σ curves, at equal values of ϵ_p. This important finding is related to the choice of the mix characteristic. The assumptions were (a) linearity with regard to stress and (b) a linear log-log relationship. From the derivation, it can be seen that the second assumption has led to this more or less unexpected result. For, when the ϵ-N relationship of equation 6 is replaced by $\epsilon = cN^a f(\sigma)$, the derivation does not change essentially. It also indicates that, for the small number of mixes for which the linear log-log approach is not accurate enough, the derived formula 17 may not be used. It is not even correct to divide the ϵ-N curve into different parts characterized by different slopes, and use the derived formula with different values of a.

Returning to the starting point, in which the general wheel-load spectrum (Figure 4) was considered, this spectrum can be divided into k classes of different stresses. For this the general formula is

Figure 4. Wheel-load spectrum.

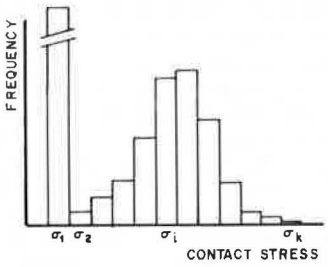

Figure 5. Simplified wheel-load spectrum.

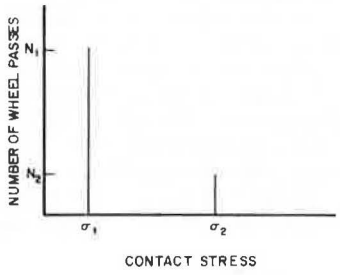

Figure 6. Random sequence of σ_1 and σ_2.

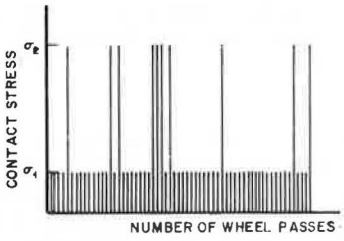

Figure 7. Compound block loading.

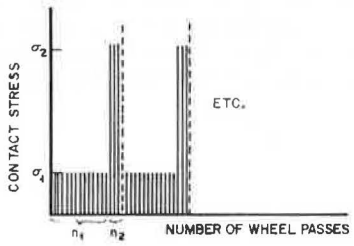

Figure 8. Procedure to determine permanent deformation under the influence of different loadings.

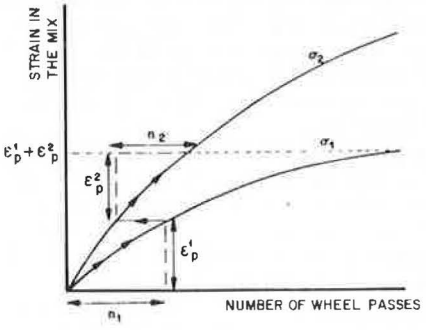

Figure 9. Special case of ϵ-N relationship: $\epsilon = c\,\sigma\,N^a$.

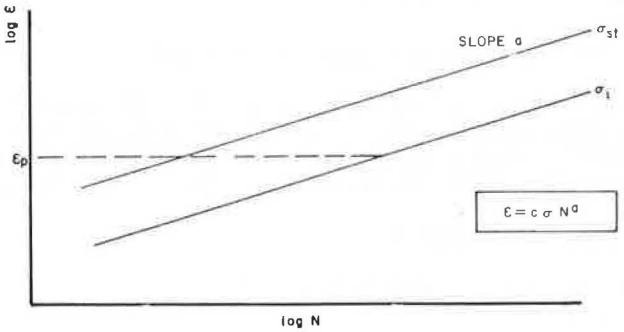

$$N_{eq} = N_{st} \sum_{i=1}^{k} (\sigma_i/\sigma_{st})^{1/a} (n_i/n_{st}) \quad (18)$$

In this formula σ_{st} can be chosen arbitrarily.

From creep and rutting experiments it has been found that the coefficient a (slope of the mix characteristic) varies between 1/3 and 1/6; hence the power 1/a varies between 3 and 9.

Formula 18, which has general validity, has been derived for the most simple case of constant temperature, constant wheel speed, and constant geometry. In this case, the strain in the mix can be calculated directly by

$$\epsilon = c \left\{ \sum_{i=1}^{k} \sigma_i^{1/a} N_i \right\}^a \quad (19)$$

In all other cases N_{eq} must be used in equation 1.

This value may be used to calculate $S_{bit,\,visc}$ (see equation 1). In formula 18, σ_{st} must be used instead of σ_0. The derivation assumes that the contact area between the tire and the pavement does not change with varying wheel loads. The geometric correction factor Z is then a constant, and the radius of the contact area R can be that of the standard wheel. However, this is not realistic and requires further consideration.

Varying Contact Area

With road vehicles, the contact area between the tire and the pavement increases with increasing wheel load and increasing contact stress. Hence, at a given layer thickness H_0, the geometric factor Z, which is a function of R (Figure 2), will depend on the contact stress, which means that the average stress under the wheel is not linearly proportional to the contact stress. De Henau (10) has investigated the relation between the contact stress and the radius of the contact area between the tire and the pavement. This relation, which is based on experimental average results, can be approximated by

$$R = c\sigma_0^{2/3} \quad (20)$$

To calculate the average stress in a given construction, equation 4 can be written as

$$\sigma_{av} = Z(R)\sigma_0 \quad (21)$$

An example of the functional relationship between Z and R is given in Figure 2. For small values of R ($R/H_0 < 1/2$), Z is proportional to R; at high values of R, Z is almost independent. Equations 20 and 21 can be combined into

$$\sigma_{av} = c\sigma_0^b \quad (1 < b < 2/3) \quad (22)$$

This equation shows that the average stress under actual traffic loads is greater than proportional to the contact stress.

If the choice of the standard wheel and the derivation of the Z-value belonging to this wheel are arbitrary, the expression of the whole wheel-load spectrum in standard wheel loads will lead to an overestimation of the lower stresses and an underestimation of the higher ones. It is very complicated to quantify this exactly. However, with a proper choice of the standard wheel there is no need to correct for this effect. If the wheel pertaining to the standard 80-kN AASHO axle load, which is in the middle of the wheel-load spectrum, is chosen, the over and underestimations are about equal and the error is negligible. For this wheel, R = 105 mm and $\sigma_0 = 0.6$ MN/m².

The same reasoning is valid with respect to the loading time of one wheel pass: t_0 is proportional to the ratio of the length of the contact area to the wheel speed. If the contact area varies, t_0 varies in the same way, and choosing the standard wheel in the middle of the load spectrum will give compensating over and underestimations.

Lateral Distribution of Wheel Loads

Actual traffic does not move in a single wheel path, but is laterally distributed over the traffic lane (11). The effect of this is twofold. First, in the calculation procedure, the interest is in the reduction in layer thickness in the middle of the rut (the deepest part), but because of the lateral distribution, the real number of wheel passes in the middle will be lower than the total number. Second, some of the material that is pushed sidewards to the lateral swelling is also pushed backwards by the wheels moving along the edge of the central wheel path.

Figure 10 gives an example of a frequency distribution of passages of the middle of a wheel. This shows that, if the interval width is smaller than the width of the tire, a wheel pass in one interval also covers the adjacent interval(s). For example, if the interval width is equal to the tire width, the adjacent interval is located in the lateral swelling, whereas if the interval width is one-third of the tire width, the two adjacent intervals are also under the passing wheel.

As the frequency distribution of the lateral displacements is based on a very large number of wheel passes, the interval width must be chosen to be small in comparison with the tire width. The tire width can be taken as the diameter of the contact area of the standard wheel, or for dual wheels, as twice this value.

The following assumptions are made.

1. No aftercompaction takes place. This means that all of the material that is pushed downwards in a rut must be moved laterally to a swelling. Deformations caused by aftercompaction will be added to the purely viscous deformations.
2. The width of a swelling is equal to the width of the rut. This assumption is derived from laboratory test track studies. Since the volume of the rut is equal to the volume of the two lateral swellings, the average height of the swelling is half the permanent deformation in the rut.
3. Since the deformations occurring in the ruts and in the swellings are both related to a combination of compression and tension, which are shear forces, no distinction will be made between the two effects in the physical sense.
4. The number of wheel passes located in the intervals under the wheel is counted as positive, and the number of wheel passes located in the swelling intervals is counted as negative and weighted by a factor of 1/2. [With a small number of wheel passes, the resulting deformation depends on the question of whether an interval is first located in a swelling and afterward under the wheel, or, with an equal number of wheel passes, is deformed in the opposite order. With a large number of randomly applied wheel passes, this influence diminishes. This means that material subjected to a number of swelling deformations that is twice the number of deformations under the wheel will not show any resulting deformation. Only a net number of load applications (positive or negative) will cause permanent deformation.]
5. The deformations in the rutting part are calculated with the formula

$$\epsilon_r = c N_i^a \quad (23)$$

Figure 10. Average lateral distribution of lorry wheels.

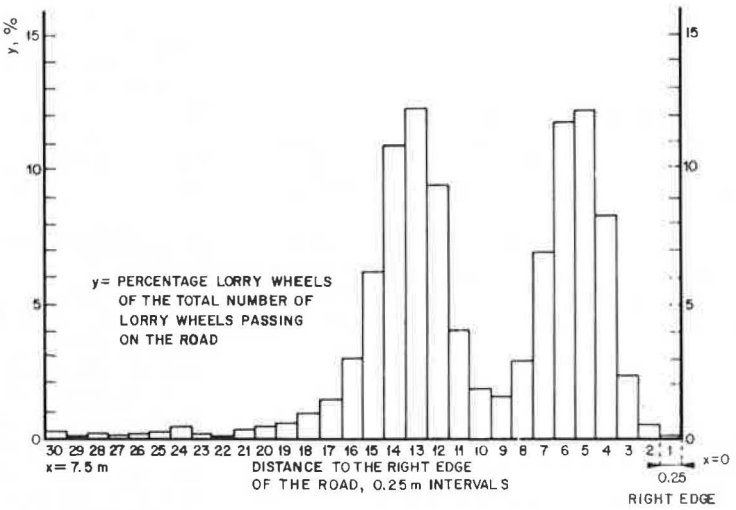

Figure 11. Calculated average deformation profiles (A and B) and profile measured on a rutted road in Holland (C).

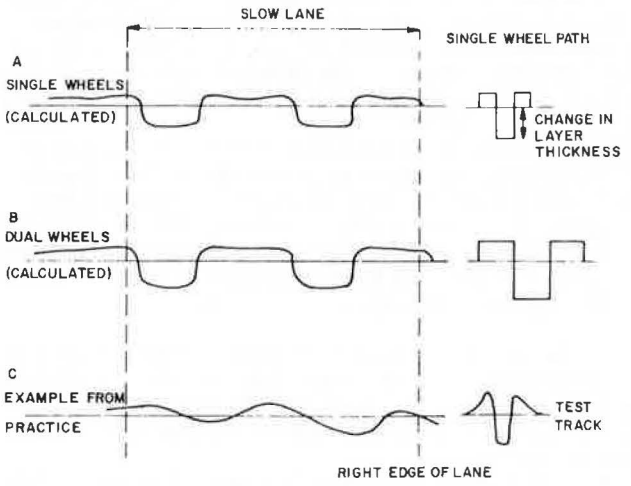

6. The deformations in the swelling part are calculated with the formula

$$\epsilon_s = \tfrac{1}{2}c(2N_j)^a \qquad (24)$$

The factor $\frac{1}{2}$ is based on assumption 2. The factor 2 in the term $(2N_j)$ is explained as follows: As explained in assumption 4, all load applications in a swelling interval are weighted by a factor of $\frac{1}{2}$ and the net number of passages in the swelling, N_j, causes the actual deformation, beginning with the zero state. From the case of a single wheel path, the swelling deformation can be calculated by the formula $\epsilon = \frac{1}{2}c\,N^a$, in which a wheel pass is given its full weight. The same must also hold for the net number of passes N_j and means that N_j must be multiplied by a factor of 2.

In the calculation procedure, the interval width was chosen as 25 mm; the width of a single wheel was taken equal to 9 intervals (225 mm); and the width of a dual wheel was taken equal to 17 intervals (425 mm). In the case of a single wheel and a material characteristic having a slope of $a = \frac{1}{6}(\epsilon = c\,N^{1/6})$, the rut depth, defined as the difference between the highest part of the swelling and the lowest part inside the rut, is 90 percent of the change in layer thickness, calculated with all wheels moving in a single wheel path (Figure 11A). When a dual wheel is applied, the rut depth is 114 percent of the change in layer thickness calculated with all dual wheels in a single wheel path (Figure 11B). If the lateral swelling is taken into account in the case of a single wheel path, these values are 60 and 76 percent respectively of the rut depth. However, it is easier to use the values of change in the layer thickness, because these values can be calculated with equation 3. If $a = \frac{1}{3}$ (an extremely unstable mix), the rut depth values are 56 and 88 percent respectively of the change in layer thickness in a single wheel path. For the combination of single and dual wheels that is found in practice, for an average mix, the rut depth (the top of the swelling to the bottom of the rut) is roughly equal to the change in layer thickness when all of the wheels move in a single wheel path.

In Figure 11 the derived average deformation profiles are compared with the measured profile of an arbitrarily chosen, strongly rutted road in Holland. The fact that the calculated profiles are more angular in shape than the measured profile is explained by the fact that at low numbers of load applications the measured deformations are lower than the values calculated by the relation $\epsilon = c\,N^a$. An actual profile of a single wheel path in a test track (also shown in Figure 11C) shows a smoother appearance than the profile used in the calculation.

Influence of Varying Temperatures and Temperature Gradients

When rut depth is to be predicted over a period of many years, the calculations must use average temperatures, for example, the mean monthly temperatures (12). Equation 1 then becomes

$$S_{bit,visc} = 3/\sum N t_0 (1/\eta)_{av} \qquad (25)$$

where

N = total number of standard wheel loads over the period of one month, and
$(1/\eta)_{av}$ = average of the reciprocal viscosities in that month.

The latter quantity is not equal to the reciprocal of the average viscosity, and thus, because η is a nonlinear function of T (see Figure 3), not equal to the reciprocal value of the viscosity at the average temperature. Thus

$$(1/\eta)_{av} \neq 1/\eta_{av} \neq 1/[\eta(\text{at } T_{av})] \qquad (26)$$

As to the question of which value to choose for η, the following should be noted. In a laboratory test track, where the temperature can be controlled, the asphalt layer may have an almost uniform temperature. In practice, or on an open-air test track, large temperature differences between the top and bottom of the layer can occur. In this case, the average viscosity must be calculated through the asphalt layer rather than the viscosity at the average temperature through the layer. The effect of temperature gradients can be seen in Figure 3, which shows that a temperature difference of 10°C causes a change in viscosity of a factor of 10.

Depending on the required accuracy, a layer can be divided into various sublayers having different temperatures, and the dynamic modulus for each sublayer can be determined. Then the stress and the $S_{bit,\,visc}$ values can be calculated with the computer program BISAR. The deformation of each sublayer can be calculated from the creep curve in the same way as in the case of one layer, and finally, all of the contributions can be summed. This refinement may be necessary when large viscosity gradients coincide with large stress gradients.

ACKNOWLEDGMENT

I am indebted to my colleagues in the Koninklijke/Shell-laboratorium, Amsterdam, especially E. de Hilster, and in Shell laboratories and offices in several other countries, for valuable discussions and assistance.

REFERENCES

1. Streuungen der Prüfergebnisse von bituminösen Mischgut. Eine Ringuntersuchung der Strabag-Bau A.G. Strabag-Bau A.G.
2. Jaarverslag Stichting Studie Centrum Wegenbouw. 1974.
3. J. F. Hills. The Creep of Asphalt Mixes. Journal of the Institute of Petroleum, Nov. 1973.
4. J. F. Hills, D. Brien, and P. J. van de Loo. The Correlation of Rutting and Creep Tests on Asphalt Mixes. Journal of the Institute of Petroleum, Paper IP 74-001, Jan. 1974.
5. P. J. van de Loo. Creep Testing, a Simple Tool to Judge Asphalt Mix Stability. Proc., AAPT, Vol. 43, 1974, p. 253.
6. P. Ugé and P. J. van de Loo. Permanent Deformation of Asphalt Mixes. Proc., Canadian Technical Asphalt Association, Vol. 19, 1974.
7. M. G. F. Peutz, H. P. M. Van Kempen, and A. Jones. Layered Systems Under Normal Surface Loads. HRB, Highway Research Record 228, 1968, pp. 34-45.
8. D. L. De Jong, M. G. F. Peutz, and A. R. Korswagen. Computer Program BISAR. Layered Systems Under Normal and Tangential Surface Loads. Koninklijke/Shell Laboratorium, Amsterdam, External Report AMSR.0006.73, 1973.
9. W. Heukelom. An Improved Method of Characterizing Asphaltic Bitumens With the Aid of Their Mechanical Properties. Proc., AAPT, Vol. 42, 1973, p. 67.
10. A. de Henau. Véhicules et circulation dans le cadre du dimensionnement des chaussées. La Technique Routière, Vol. 12, No. 1, 1967, p. 1.
11. A. de Henau. Analyse de la circulation dans le cadre du dimensionnement des chaussées. La Technique Routière, Vol. 12, No. 4, 1967, p. 35.
12. J. M. Edwards and C. P. Valkering. Structural Design of Asphalt Pavements for Road Vehicles—the Influence of High Temperatures. Highways and Road Construction, Feb. 1974.